A major purpose of the Technical Information Center is to provide the broadest dissemination possible of information contained in DOE's Research and Development Reports to business, industry, the academic community, and federal, state and local governments.

Although a small portion of this report is not reproducible, it is being made available to expedite the availability of information on the research discussed herein.

1

LA-UR-83-3658

CONF-840813--1

Los Alamos National Laboratory is operated by the University of California for the United States Department of Energy under contract W-7405-ENG-36

LA-UR--83-3558

DE84 004415

TITLE: A TRAC-PF1 ANALYSIS of LOSS-OF-FLUID TEST L6-7/L9-2

AUTHOR(S): John K. Meier

NOTICE
PORTIONS OF THIS REPORT ARE ILLEGIBLE.
It has been reproduced from the best available copy to permit the broadest possible availability.

SUBMITTED TO: 1984 ANS/ASME Nuclear Power Engineering Conference
Portland, Oregon
August 5-8, 1984

Los Alamos
Los Alamos National Laboratory
Los Alamos, New Mexico 87545

A TRAC-PF1 ANALYSIS OF LOSS-OF-FLUID TEST L6-7/L9-2*

John K. Meier
Safety Code Development Group
Energy Division
Los Alamos National Laboratory
Los Alamos, NM 87545

The Los Alamos National Laboratory is developing the Transient Reactor Analysis Code (TRAC-PF1) to provide the capability for advanced best-estimate predictions of postulated accidents in pressurized-water reactors (PWRs) and for many thermal-hydraulic experimental facilities.

As part of our independent assessment of TRAC-PF1, we analyzed Loss-of-Fluid Test (LOFT) L6-7/L9-2 and compared the test data to the calculated results. Test L6-7 simulated a cooldown transient similar to the Arkansas Nuclear One Unit-2 turbine-trip transient. During the L9-2 phase of the test, the primary-coolant pumps were tripped and natural circulation cooled the core while the plant cooldown continued. The TRAC results matched the test data well during the L6-7 portion of the transient (0.0-324 s). However, during the L9-2 portion the calculated natural-circulation flow rate in the intact loop was much higher than the measured rate.

Other analysts have encountered a similar problem in their calculations of this test, and they attribute the deficiency to a difference between the calculated and the actual value of the LOFT locked-rotor pump resistance. However, the test data exhibit a multidimensional fluid-temperature distribution in the downcomer and imply a multidimensional flow field in the downcomer. We believe that the temperature distribution reduces the driving head for natural circulation. This may have implications for pressurized thermal-shock (PTS) transients in full-scale reactors.

The calculated vessel and valve leakage rates during natural circulation have large uncertainties. Also, significant uncertainties in the actual steady-state leakage rates, which were used as a basis for these calculations, probably compound the problem.

---

*This work was funded by the USNRC Office of Nuclear Regulatory Research, Division of Accident Analysis.

The primary-system pressure comparison is the most significant. From 300-400 s, the system pressure was very sensitive to the amount of water remaining in the pressurizer when the pumps tripped. After 500 s the system pressure was sensitive to the leakage rate in the reflood-assist bypass valves (RABVs) during the early portion of the transient. For a reasonable match between the test and the calculated results, we decreased the RABV leakage rate to 50% of the approximate values given by the Idaho National Engineering Laboratory (INEL). Otherwise, the comparison between the test data and calculated system pressure was good.

The analysis showed that very detailed noding is required in several locations to avoid numerical diffusion of liquid energy in the slowly moving liquid. It was important to calculate the correct distribution of energy in the system to obtain the correct distribution of vaporizing fluid.

The gradual system cooling during Test L9-2 led to a phenomenon that would not occur during a natural-circulation test at a constant temperature. During the later portion of the transient, the heat addition from the vessel walls was greater than that from the core. The complex flow patterns that probably resulted from this phenomenon indicate that a three-dimensional vessel model may yield better results than the one-dimensional model used in these calculations.

An error in TRAC-PF1 was discovered that could result in an inaccurate heat-transfer area on a tee side branch. The error was limited to situations where an annulus was involved (such as a downcomer or leakage flow path). The error is corrected in TRAC-PF1/MOD1.

The calculated steady-state pressure drops in the vessel were improved significantly over previous one-dimensional analysis of the LOFT system. We accomplished this improvement by changing all the tee components such that the main branch of the tee was used to model the main flow path.

The details of the test, analysis and data comparisons are presented in the following sections. There, we

- describe the test apparatus,
- describe the experiment and experimental phenomena,
- describe the TRAC input,
- present and discuss the data comparisons, and
- provide details of computer use.

Test Apparatus

The LOFT facility (shown in Fig. 1) is a 50-MW(t) PWR, detailed descriptions of which may be found in Refs. 1, 2, and 3. The description presented here will be limited to the particular configuration of the facility used for experiment L6-7/L9-2, as well as specific details of the facility particularly important to this experiment.

The reflood-assist bypass lines (RABL) were particularly important in Test L6-7/L9-2. These lines connect the broken hot and cold legs of the LOFT system through the RABV. These valves leak at a rate such that fluid in the

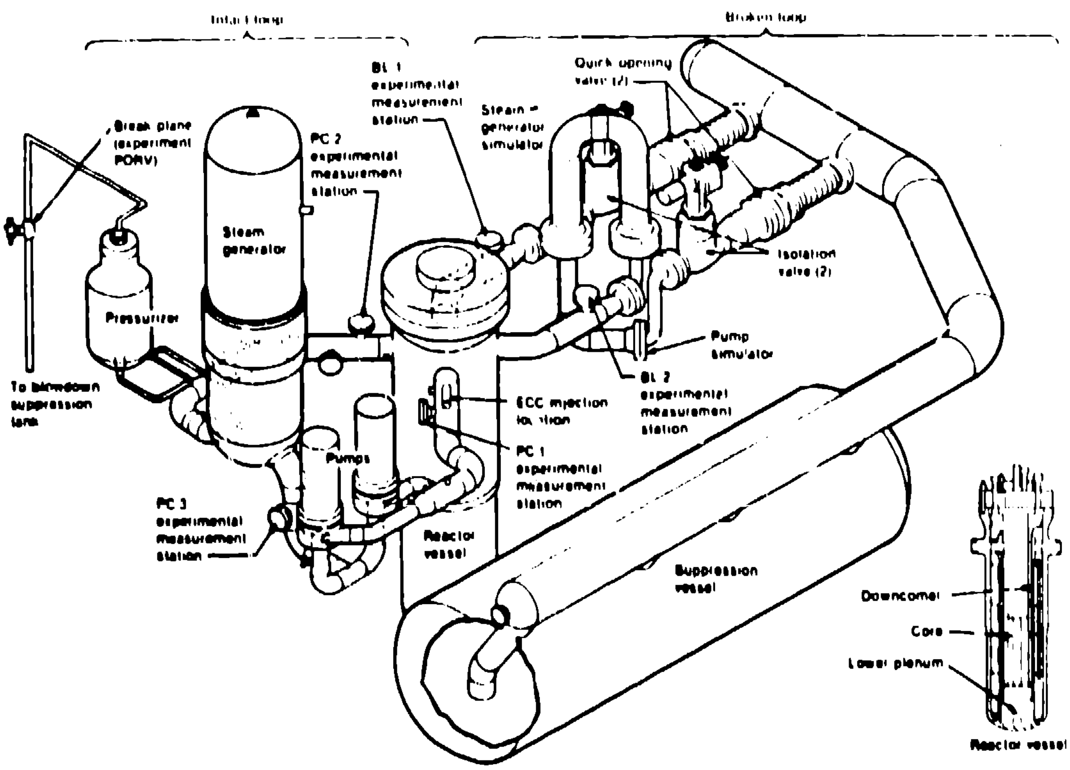

Fig. 1.
LOFT facility diagram (Ref. 3).

lines heats during steady state but only partially cools during the transient. This trapped hot fluid constitutes the major source of steam generation during the latter part of Test L9-2.

The leakage paths in the vessel were very important during this test because they influenced the flow fields and temperature distribution in the vessel.

The two most important ones were: (1) the gap between the downcomer filler and pressure vessel in which we calculated the fluid to flow upward during natural circulation and (2) the leakage between the hot and cold legs carrying 5% of the primary-system flow during pump operation and as much as 20% of the system flow during natural circulation. In this test, most of the broken hot leg was removed and the warm-up recirculation lines were closed.

Experimental Phenomena

A description of the important events and phenomena in these tests is presented below. These events may be followed in the primary-system pressure trace of Fig. 2. The experiment begins as the operator manipulates the steam-generator secondary-side flow-control valve to give a predetermined rate of steam flow. After the reactor is manually scrammed at 7 s, this rate of flow cools the secondary-system fluid and consequently the primary-system fluid.

The fluid in the primary system shrinks, drawing water out of the pressurizer and lowering the pressure in the primary system. This situation continues until the pressurizer almost empties and the primary-coolant pumps trip.

Note that while the pump is running there is small leakage through the RABV, resulting in cooled fluid in the broken loop and RABL. Also, some fluid in the upper head is cooled as a result of fluid movement in the upper plenum.

As the hot, saturated fluid in the pressurizer is injected into the hot leg, it mixes with the colder fluid in the system. Therefore, when all the fluid in the pressurizer is injected, no saturated fluid in the primary system remains; further vaporization is precluded. This causes the primary-system pressure to drop rapidly at around 300 s. Next, the flow rate in the intact loop drops with the coastdown of the pumps, resulting in a greater temperature difference across the vessel. This causes the temperature of the intact hot leg to rise temporarily, with a resulting temporary rise in the primary-system

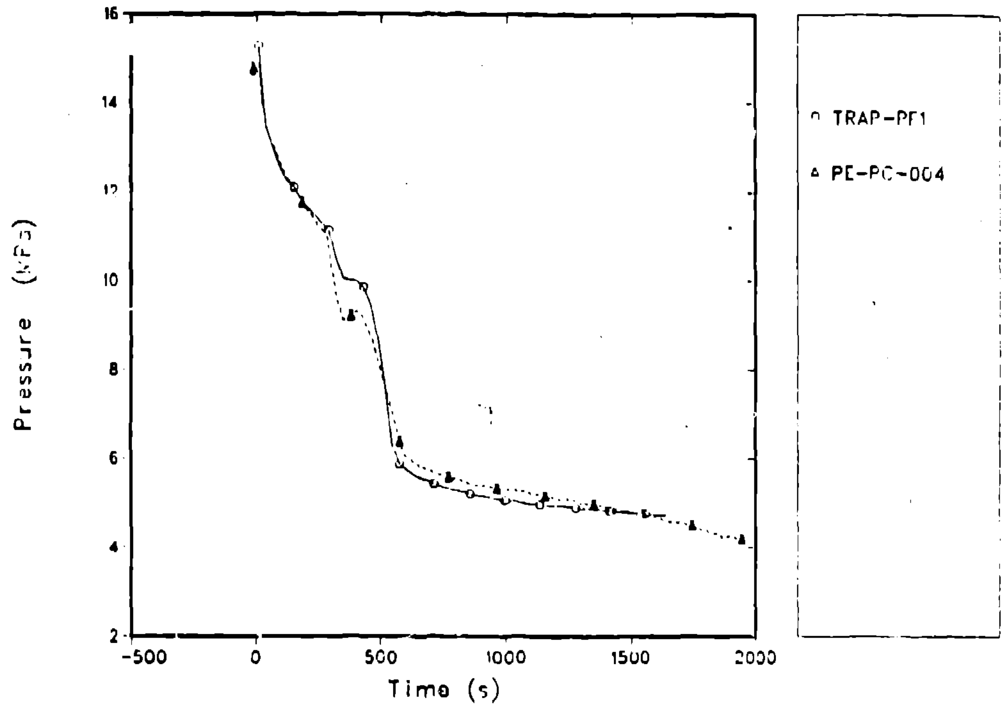

Fig. 2.
Primary-system pressure.

pressure. This temperature difference establishes natural circulation in the intact loop that limits intact-loop heating and eventually lowers the system pressure again at around 400 s.

The experiment data indicate that the natural-circulation patterns during this time are very complicated. For instance, thermocouples located in the downcomer show it to be as hot as the core. The TRAC calculation suggests the presence of significant mass flow in the various leakage paths within the vessel. Also, a heat balance across the vessel indicates that well over half of the heat added to the fluid passing through the vessel is from the metal structure. Note that if the fluid temperature in the system as a whole were not decreasing, the fluid and the structure would be the same temperature and the vessel flow patterns might be much different. The system pressure continues to fall as the primary-system fluid cools; then, at 600 s, liquid in the upper head and then in the RABL starts to vaporize, stabilizing the pressure for the rest of the ...

Description of TRAC Input

A component diagram of the input description is presented in Figs. 3 and 4.

The input description used for these analyses was derived from the one used for the L9-1/L3-3 analyses. An important difference was that three of the tees used to model the vessel were changed. The change was such that the main branch of the tee was used to model the main flow path of the fluid. In the previous model, where the main flow path of the fluid passed through the side branch of the tee, the steady-state pressure drop was seriously overpredicted because of the way the momentum source term is handled at a tee junction.

Another significant change was that the broken loop and RAbL were noded much more finely. In the previous input description, only one or two volumes were used to model each of these sections of piping. Cold water from the main system, which slowly entered the broken loop due to RABV leakage, was quickly transported by numerical diffusion throughout the broken loop and RABL. In the actual test, this colder fluid appeared to remain near the entrance to the

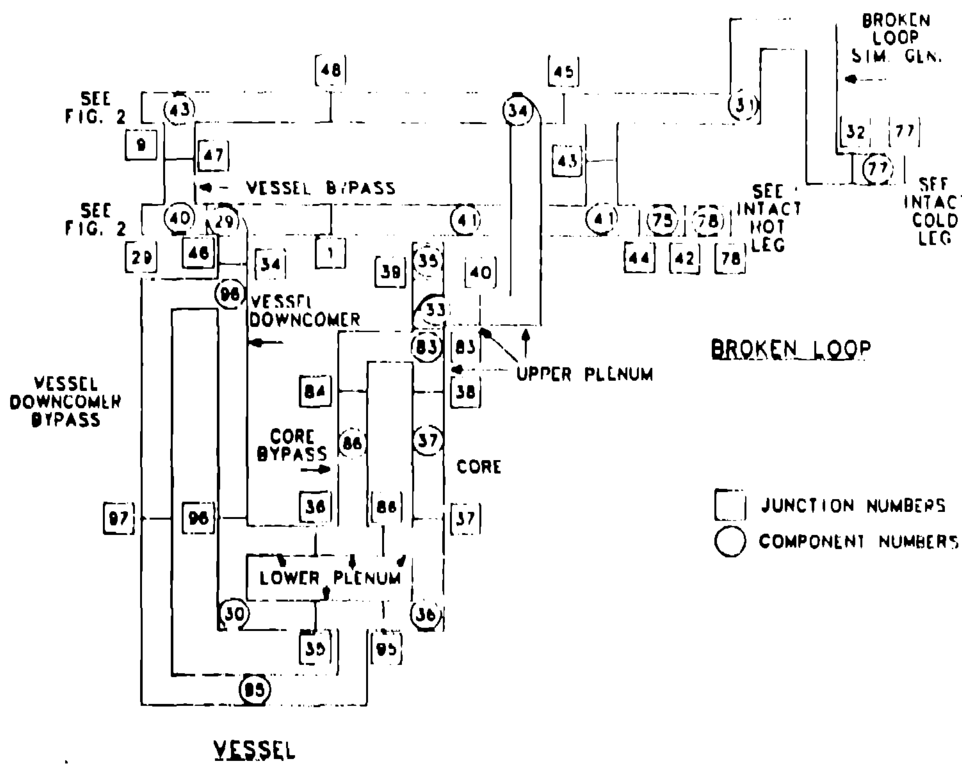

Fig. 3.
Vessel and broken-loop component diagram.

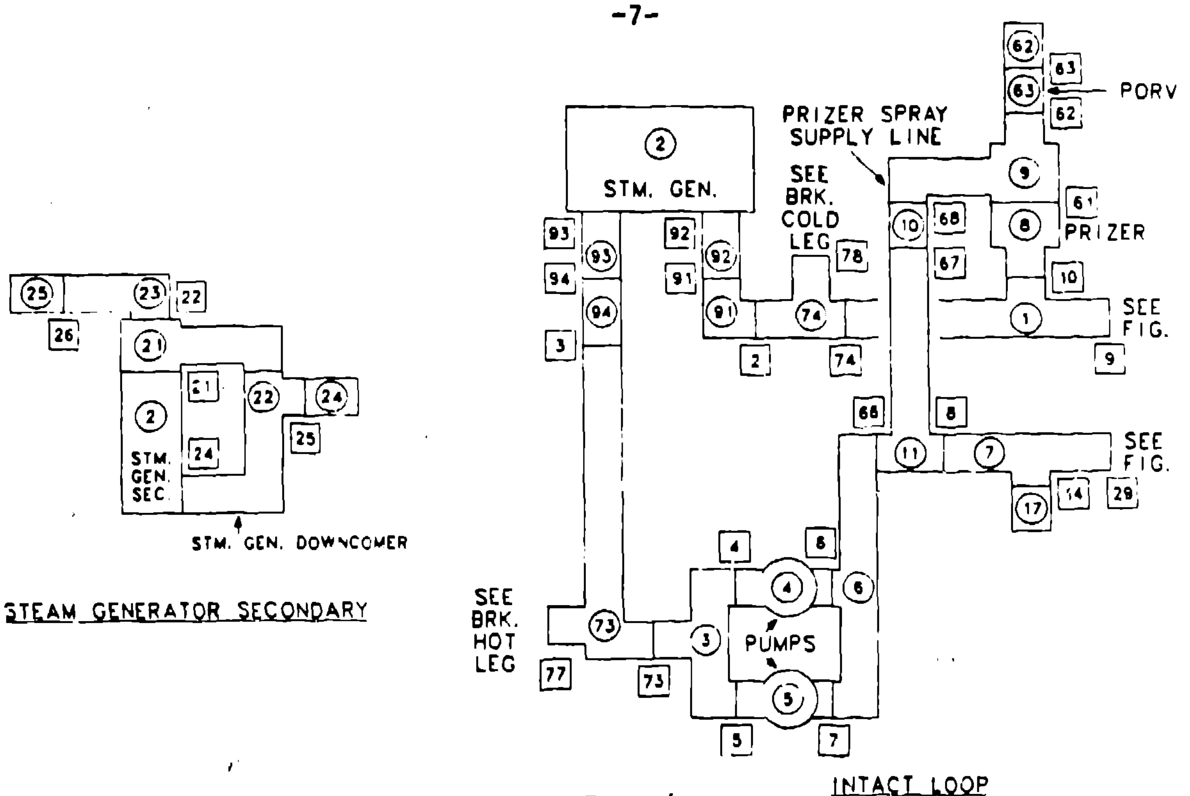

Fig. 4.
Intact loop component diagram.

broken loop. By using much finer noding, we minimized this numerical diffusion. In the final description, [illegible] to 10 volumes were used to model each of these components. Other changes from the L9-1/L3-3 model were that the power-operated relief valve (PORV), the warm-up recirculation valves, and much of the broken-loop hot leg were removed.

The error found in the heat-transfer area on the side branch of a tee is related to the method used to model annuluses such as the downcomer and leakage flow paths. In these situations, the heat-transfer area is much greater than would be the case for a pipe with the same flow area. In TRAC a separate pipe radius is input to be used only for heat transfer. The error was that TRAC was not using this radius in the side branch of the tee to calculate the heat-transfer area but was calculating a wall area based on the volume and length of the tee-side branch.

To conserve computer time, the particular input description in these analyses uses a one-dimensional vessel description. The test data and the analytical results together indicate that important three-dimensional effects are present in the vessel, especially in the downcomer.

The primary boundary condition used in the analysis was that pressure in the steam-generator secondary-side was controlled by a time-dependent break. Use of a fill to match the steam-generator secondary-side outlet mass flow was considered but rejected based on the superior accuracy of the pressure data.

The initial pressurizer liquid level was fixed at the lowest value within the error band of the experimental data.

Simulation of the leakage paths within the vessel presented special modeling problems. Because of the intricate geometry of these paths, they are modeled empirically. That is, a parameter within the TRAC input description is adjusted until TRAC calculations of the steady-state leakage rate match the INEL-supplied data. The three changeable parameters are the flow area, the hydraulic diameter, and the friction factor. A problem encountered in this test was that the range of flow rates in these leakage paths is many orders of magnitude. Therefore, none of the above methods is likely to remain valid when natural circulation drives the flows in the system. Furthermore, the direction of the flow in several of the leakage paths reverses under natural-circulation conditions.

There is also some question as to whether the specified steady-state value of leakage for the RABVs is applicable to this particular test. The calculations of Test L6-7/L9-2 were significantly improved when the leakage rate was halved.

In these tests, the one-dimensional vessel model presented a problem regarding the upper head. Because the upper head is modeled as a dead-end stub of pipe, there is little circulation between it and the rest of the system until it begins to flash. In the experiment, there is actually a small degree of circulation of fluid in the upper head due to jets of fluid from the upper plenum, an additional indication of multidimensional behavior. This circulation lowers the temperature of the fluid in the upper head during the first 400 s of Test L6-7. To account for this temperature decrease in the calculation, the fluid in the upper head was set at a lower initial temperature than recorded in the test data.

Presentation and Discussion of Data Comparisons

The principal boundary condition used during this test was the pressure in the steam-generator secondary side. This then determined the temperature in the steam-generator secondary side, which in turn determined the temperature at the outlet of the steam-generator primary side. Not surprisingly, we see in Fig. 5 that the test and calculated results of the outlet temperature agree well.

While the pump is running, all of the temperatures in the flowing loop essentially equalize after the reactor scrams. The intact-loop hot-leg temperature presented in Fig. 6 is typical of these. During Test L6-7, the experiment and the calculated results are the same.

The data comparisons of the fluid temperatures in the broken loop and RABL were influenced strongly by the leakage rates through the RABV. The results presented here in Fig. 7 were from a run where the leakage rate was approximately 50% of the specified one.

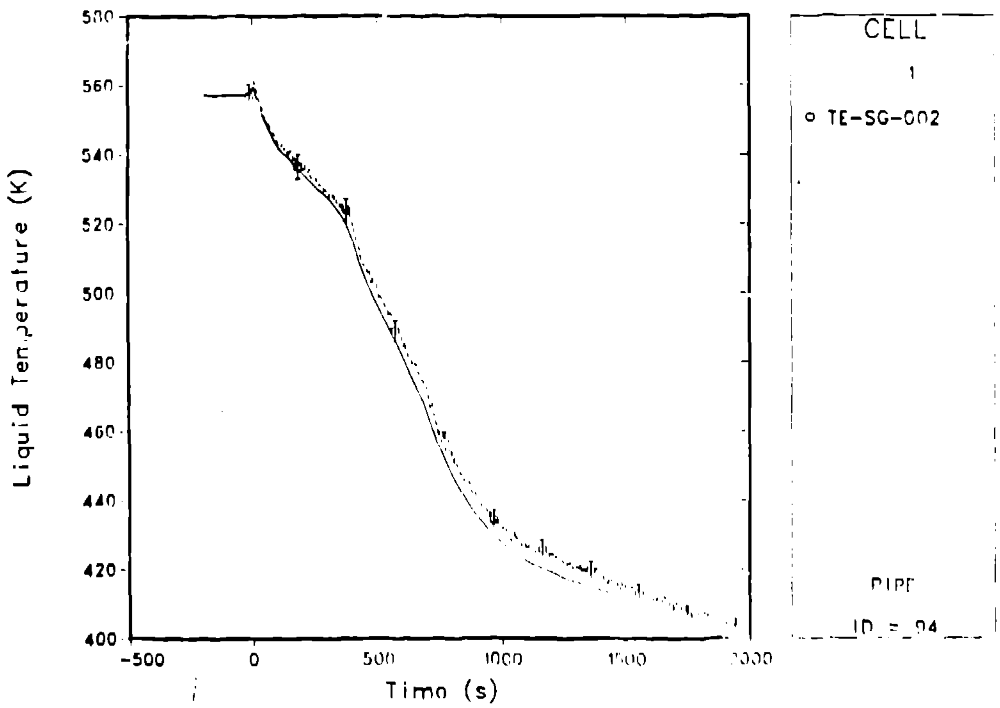

Fig. 5.
Steam-generator-outlet temperature.

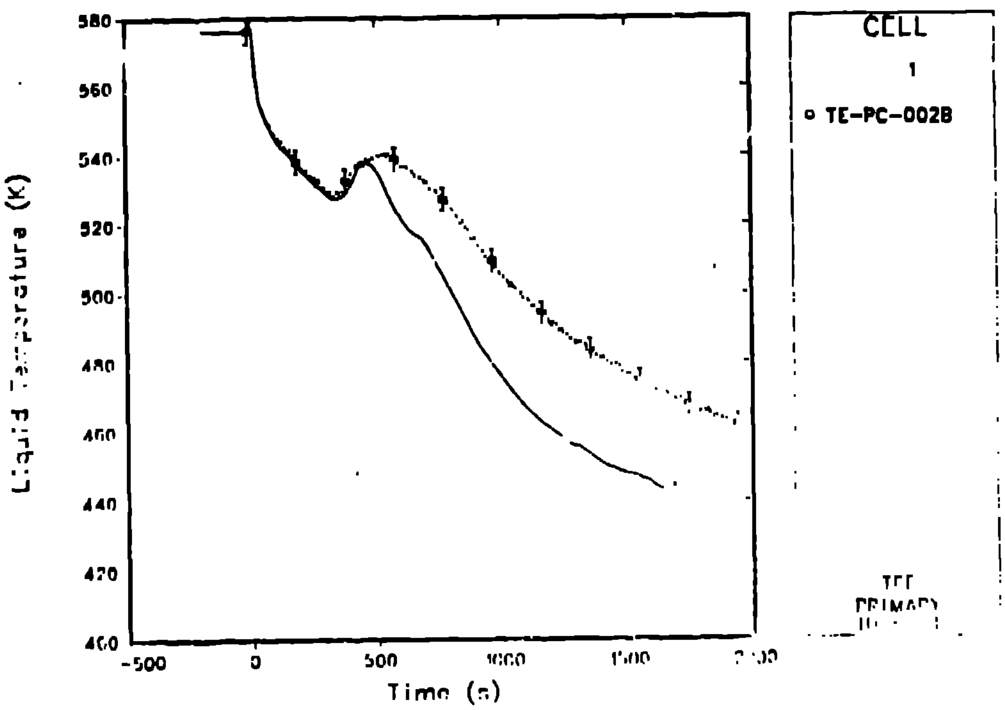

Fig. 6.
Intact-loop hot-leg temperature.

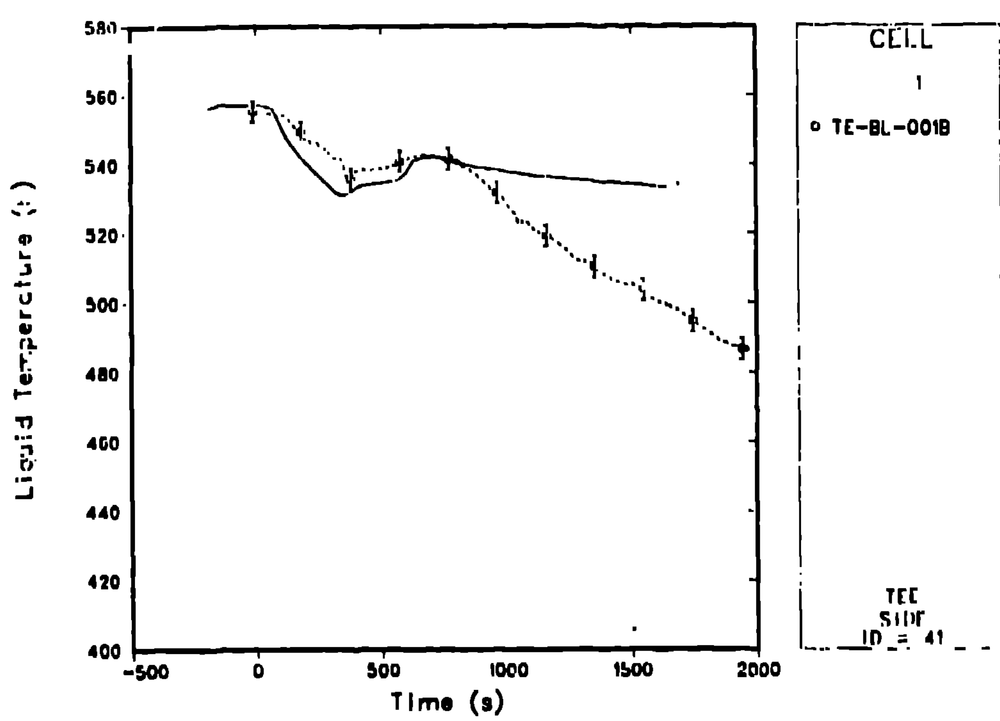

Fig. 7.
Broken-loop cold-leg temperature.

The primary-system pressure is presented in Fig. 2. The test and calculated results agree except in the 300-400-s interval. The sudden drop in pressure at about 300 s occurs when the pressurizer empties of liquid and no vaporizing liquid remains in the primary system to moderate the pressure decrease. The slight increase in pressure that occurs next results from the increase in temperature of fluid in the vessel and intact-loop hot leg when the coolant pumps coast down. Why the test and the calculated results differ is not clear, as both the emptying of the pressurizer and the coastdown of the coolant pump occur at approximately the correct time in the calculation. It is possible that the difference could relate to the fluid in the pressurizer surge line or to mixing in the upper plenum.

The relatively stable pressure after 600 s appears, at least partially, a result of vaporization of fluids in the RABL and broken loop. In initial calculations of this test using higher RABV leakage rates, the early temperature history in the RABL was significantly underpredicted. The primary-system pressure after 600 s also was underpredicted. When we roughly matched the temperature of the fluid in this loop by adjusting the leakage rates for the RABVs, we obtained reasonably good agreement between the test and calculated results. We believe vaporization of the high-temperature liquid in the upper head and downcomer also helped stablize the system pressure. Because we could not match these temperature profiles with the one-dimensional model used in this analysis, we could not determine their significances.

Turning our attention to the natural-circulation-dominated part of the transient (Phase L9-2), we clearly see in Fig. 8 that the calculated mass flow in the intact-loop hot leg is much greater than in the test data. Correspondingly, we see that, whereas the calculated steam-generator-outlet (Fig. 5) and intact-loop cold-leg (Fig. 9) temperatures match the test data, the calculated intact-loop hot-leg temperature (Fig. 6) is much lower than the test data. When we examine Figs. 10 and 11, we also see that the measured axial fluid-temperature distributions near the broken-loop cold-leg nozzle and the intact-loop cold-leg nozzle, respectively, in the downcomer are far different than those calculated in the model as presented in Fig. 12. In fact, the test data have an inverse temperature profile to that which we would expect, with the hottest fluid at the top of the downcomer (r stable thermal stratification). This is particularly surprising when one considers the small distance between the intact-loop cold-leg inlet and downcomer Stalk 2. Also, note that the temperature distributions measured by the two stalks are consistent.

A partial explanation for the inverse profile may be that much of the energy added to the fluid in the vessel is from the gap behind the downcomer, and the flow in this gap is from the bottom of the vessel to the top. Thus, the hot fluid from the gap is dumped into the top of the downcomer. Because the TRAC model used in this analysis accounted for the downcomer gap flow and still did not calculate the correct temperature profile, we believe three-dimensional flow patterns and streaming of the cold fluid from the intact-loop cold leg also are responsible for the inverse temperature profile.

The actual flow profiles in the downcomer are not known. It is probable that they are much more complicated than those predicted by the one-dimensional method used for this analysis. Another significant observation is that the temperature profile in the downcomer is similar to that in the core and thus no

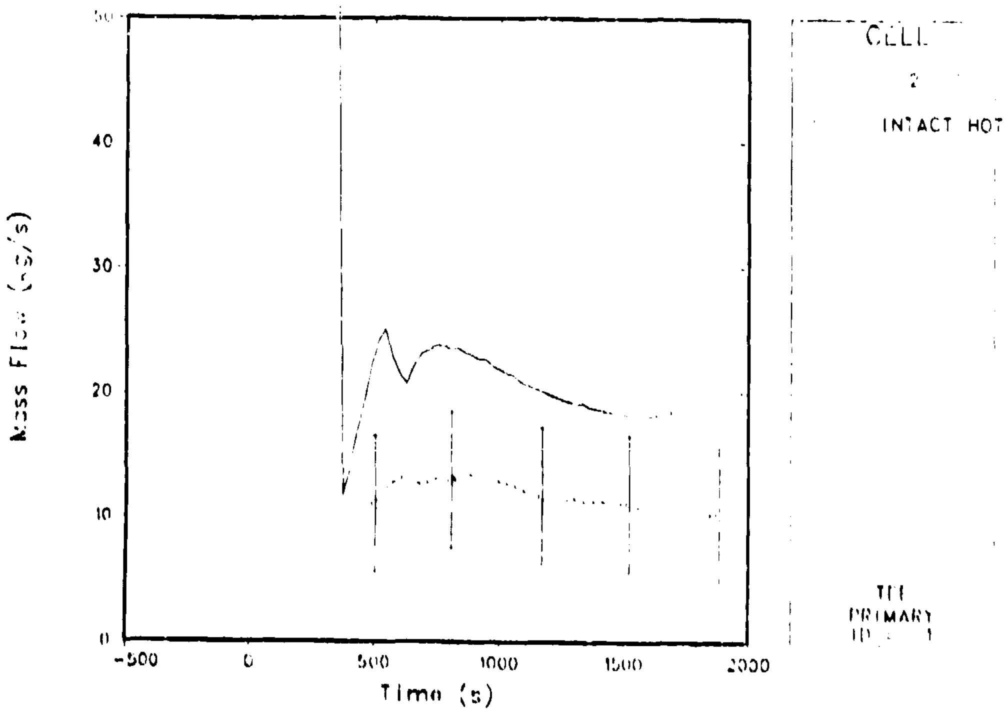

Fig. 8.
Intact-loop mass flow rate.

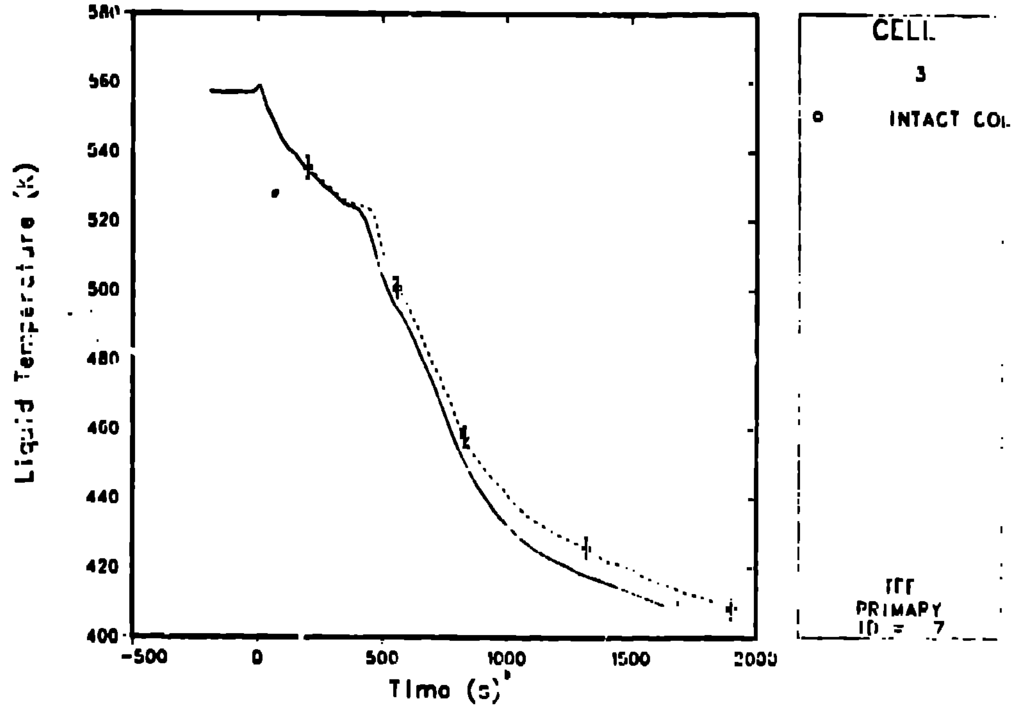

Fig. 9.
Intact-loop cold-leg temperature.

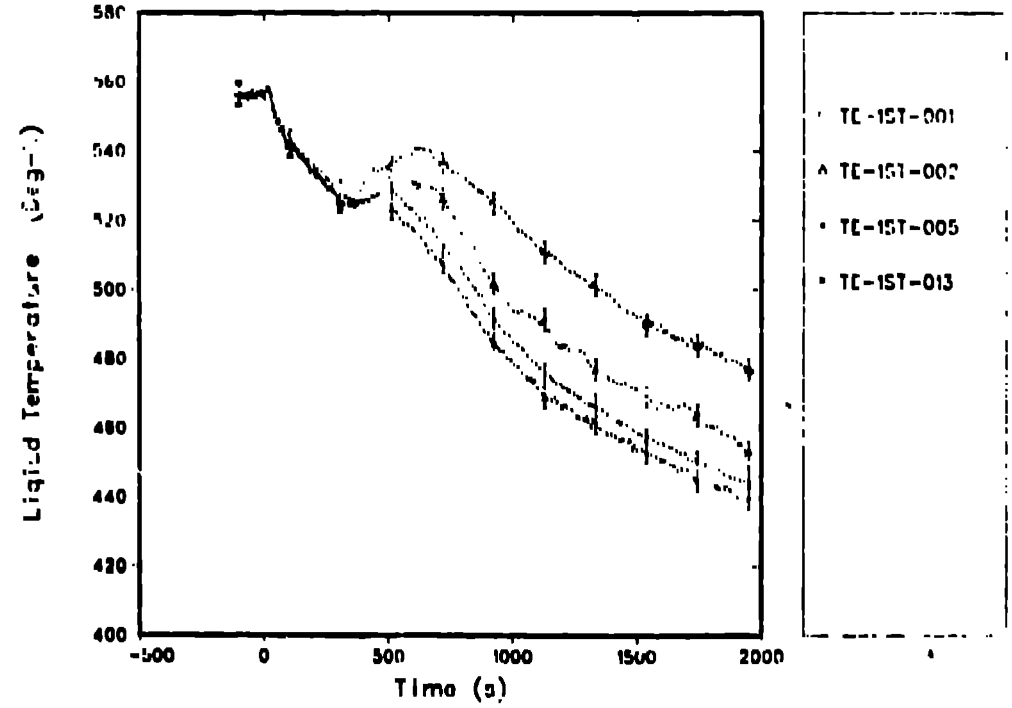

Fig. 10.
Experiment downcomer tem⸱⸱ratures (D. C. Stalk 1).

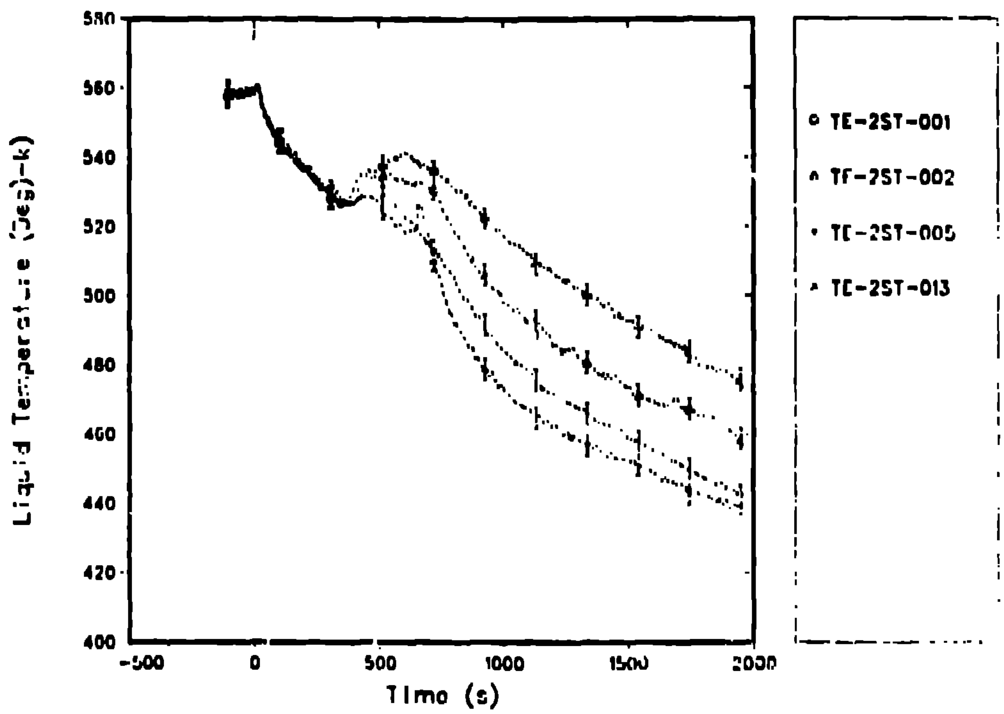

Fig. 11.
Experiment downcomer temperatures (D. C. Stalk 2).

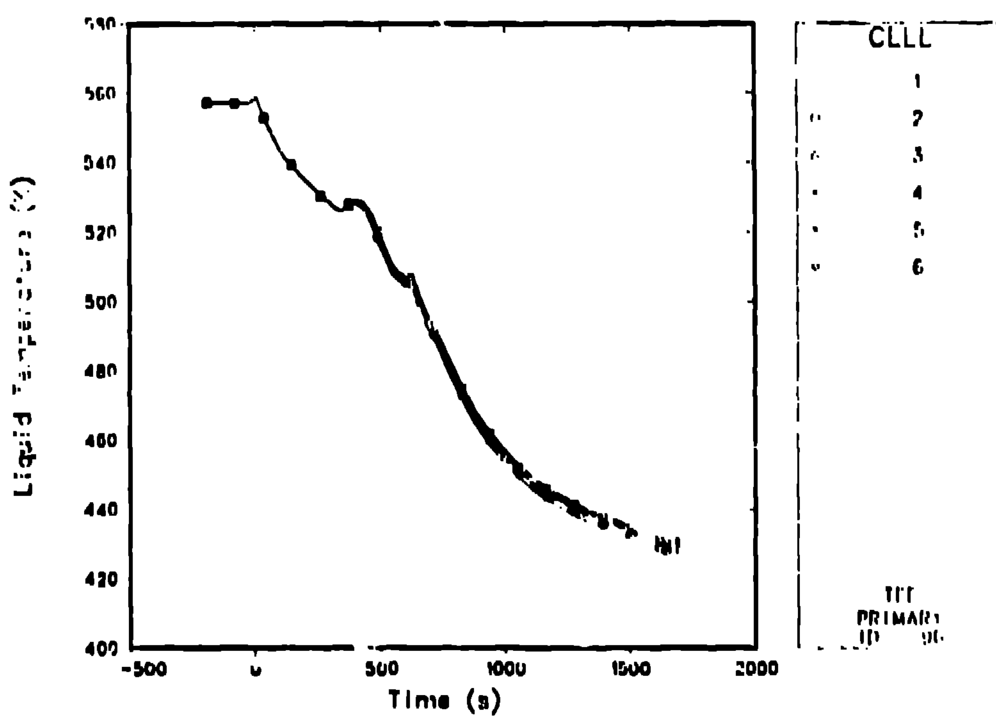

Fig. 12.
Calculated downcomer temperatures.

natural-circulation driving potential is provided by the vessel. We feel this at least partially explains the difference between the test and calculated intact-loop flow rates.

An analysis of L6-7/L9-2 was performed using an alternate input description in which the locked-rotor resistance of the pump had been increased by a factor of 10. As expected, the intact-loop flow rate and temperature were brought into line with the test data; however, another LOFT test, L6-2 (Ref. 4.), indicates that the locked-rotor resistance is not substantially in error. The primary-system pressure comparison was somewhat worse in the alternate-case downcomer.

Computer Use

The TRAC calculations of L6-7/L9-2 were performed on a Control Data Corporation 7600 computer. The steady state took 2700 s of Central-Processing-Unit time; the transient took 8200 s.

REFERENCES

1. Douglas L. Reeder, "LOFT System and Test Description (5.5-Ft Nuclear Core 1 LOCES)," Idaho National Engineering Laboratory, NUREG/CR-0247 TREE-1208, July 1978.

2. S. C. Madden, "LOFT Experiment Operating Specification Nuclear Test L6-7/L9-2," Idaho National Engineering Laboratory, EGG-LOFT-5447, June 1981.

3. Benjamin D. Stitt, Janice M. Divine, "Experiment Data Report for LOFT Anticipated Transient Experiment L-6-7 and Anticipated Transient with Multiple Failures Experiment L9-2," Idaho National Engineering Laboratory, EGG-2121 (NUREG/CR-2277), September 1981.

4. Doyle L. Baff and Janice M. Carpenter, "Experiment Data Report for LOFT Anticipated Transient Experiments L6-1, L6-2, and L6-3," Idaho National Engineering Laboratory, EGG-2067 (NUREG/CR-1797), December 1908.